Int. J. Electrochem. Sci., 14 **(2019)** 1773 – 1781, doi: 10.20964/2019.02.59

International Journal of ELECTROCHEMICAL SCIENCE
www.electrochemsci.org

Short Communication

Electrochemical Study of the Oxygen Evolution Reaction on MoNi/Carbon Fibre Electrode in 0.1 M NaOH

Tomasz Mikolajczyk[1,*], *Andrii Slis*[2], *Tetyana Solodovnik*[2]

[1] Department of Chemistry, Faculty of Environmental Management and Agriculture, University of Warmia and Mazury in Olsztyn, Plac Lodzki 4, 10-957 Olsztyn, Poland
[2]Department of Chemical Technology and Water Treatment, Faculty of Construction, Cherkasy State Technological University, Shevchenko Boulevard, 460, 18006 Cherkasy, Ukraine
[*]E-mail: tomasz.mikolajczyk@uwm.edu.pl

Received: 3 October 2018 / *Accepted:* 20 November 2018 / *Published:* 5 January 2019

The oxygen evolution reaction (OER) was investigated on pure carbon fibre CF and MoNi/CF tow electrodes in 0.1 M NaOH electrolyte at room temperature. MoNi alloy modification of CF was carried-out by electrodeposition in an electrolytic bath. The OER activity of both catalyst materials was examined by means of a.c. impedance spectroscopy and Tafel polarization techniques. The deposition of MoNi alloy on the CF material was evidenced by energy dispersive X-ray (EDX) spectroscopy; additionally, its presence had a significant influence on the recorded electrochemical parameters, such as charge-transfer resistance and exchange-current density.

Keywords: Carbon fibre; CF; MoNi alloy; impedance spectroscopy; OER

1. INTRODUCTION

In recent years, the global energy consumption has rapidly increased [1, 2], which has amplified the overall impact of non-renewable energy sources on natural environment. With respect to above ecological challenge, it is necessary to investigate alternative energy carriers. One of the most promising substitutes for fossil fuels is hydrogen produced from water electrolysis by means of the so-called *green* energy. This process is considered to be the cleanest way to make hydrogen of ultra-pure quality, as it creates zero waste [3-6]. This is because the prime processes occurring during water electrolysis are the hydrogen evolution reaction (HER) and the oxygen evolution reaction (OER) [7]. From the kinetic aspect, the OER requires more energy than the HER and higher overpotentials for the formation of oxygen molecule [8-11]. Several studies have been undertaken to find the best electrocatalyst for the OER by studying their properties (electrochemical efficiency, performance in different media, corrosion

resistivity and commercial price) [12]. Several metal oxides, such as IrO_2 and RuO_2 showed good electrocatalytic activity in acidic solutions [9, 13-16]. However, these materials could not be considered as low-cost catalysts for the OER. On the other hand, in alkaline media, some transition metals (e.g. Ni, Co, Fe and Mn) and their oxides, and oxyhydroxides present reasonable activity in an anodic reaction [17-19]. Carbon fibre (CF) is an attractive electrode material that has been examined for the use in industrial water electrolysis. The main advantages of carbon fibre material are its high surface area, good flexibility and corrosion resistance in both acidic and alkaline solutions. Therefore, carbon fibre with appropriate pre-treatment could be used as a basic material for electrode preparation [20, 21].

This work focuses on the a.c impedance and polarization measurements of the OER, performed on 12,000-filament (12K) Hexcel AS4C carbon fibre (CF) and MoNi/CF tow electrodes in 0.1 M NaOH electrolyte.

2. EXPERIMENTAL

A Millipore Direct-Q3 UV water purification system with 18.2 MΩ cm water resistivity was used to prepare all necessary solutions. The main solution of 0.1 M NaOH was prepared from AESAR, 99.996 % NaOH pellets. Atmospheric air was removed from a working electrolyte solution before experimental measurements by bubbling with high purity argon (Ar 6.0 grade, Linde). In addition, high purity sulphuric acid (SEASTAR Chemicals, BC, Canada) was used to prepare a 0.5 M H_2SO_4 solution in order to charge a Pd reversible hydrogen electrode.

In this study, a standard three-electrode electrochemical cell was used, containing a working electrode (WE) in a central part, a reversible Pd (0.5 mm diameter, 99.9 % purity, Aldrich) hydrogen electrode (RHE) as a reference and a Pt (1.0 mm diameter, 99.9998 % purity, Johnson Matthey, Inc.) counter electrode (CE), both placed in separate compartments. Working electrodes were prepared from Hexcel 12K AS4C carbon fibre tow material (12,000 individual filaments with a diameter of 7 microns each and about 26 cm^2 of geometrical area per 1 cm long ribbon). In order to remove a protective organic sizing from fresh carbon fibre, the tow electrodes were heat-treated for 4 hours at 350 °C in a muffle furnace. MoNi alloy electrochemical deposition on the CF samples was done by using an electrolytic bath consisting of the following components (concentrations in g dm^{-3}): $Na_2MoO_4 \times 2H_2O$ – 20; $NiSO_4 \times 6H_2O$ (99 % purity, Sigma-Aldrich) – 90; $C_6H_8O_7$ (citric acid, ≥99.5 %, Sigma-Aldrich) – 40; $C_6H_{11}O_7Na$ (sodium gluconate, ≥99 % Carl Roth) – 150; $Na_3C_6H_5O_7$ (trisodium citrate, ≥99 %, Sigma-Aldrich)– 50. The deposition process was carried out at a cathodic current-density of 0.5 mA cm^{-2} at 30 °C for 2 minutes to obtain a catalyst deposit at *ca.* 1.8 wt.% MoNi (with a ratio of about 1:1) [22].

The *Solatron* 12,608 W Full Electrochemical System was used to obtain experimental data from electrochemical impedance spectroscopy and quasi steady-state polarization experiments. For a.c. impedance measurements, the amplitude was set to 5 mV and the frequency swept from 1.0×10^5 to 0.5×10^{-1} Hz. Additionally, quasi-potentiostatic anodic polarization experiments (recorded at a scan rate of 0.5 mV s^{-1}) for the OER were carried-out at all electrodes. All measurements were performed at room temperature. *ZView 2.9* and *Corrview 2.9* software packages for Windows were used for data analysis, and the impedance spectra were fitted by means of a complex, non-linear, least-squares immittance

fitting program *LEVM 6*, written by Macdonald [23]. All other information about pre-treatment applied to electrochemical cell and electrodes was given in the previous publications from this laboratory [24-26].

Furthermore, a scanning electron microscope (SEM) FE-SEM Merlin unit with XFlash 5010 Bruker EDX compartment was employed for spectroscopic characterization of prepared electrodes.

3. RESULTS AND DISCUSSION

3.1. SEM and EDX characterization of MoNi/CF tow electrode

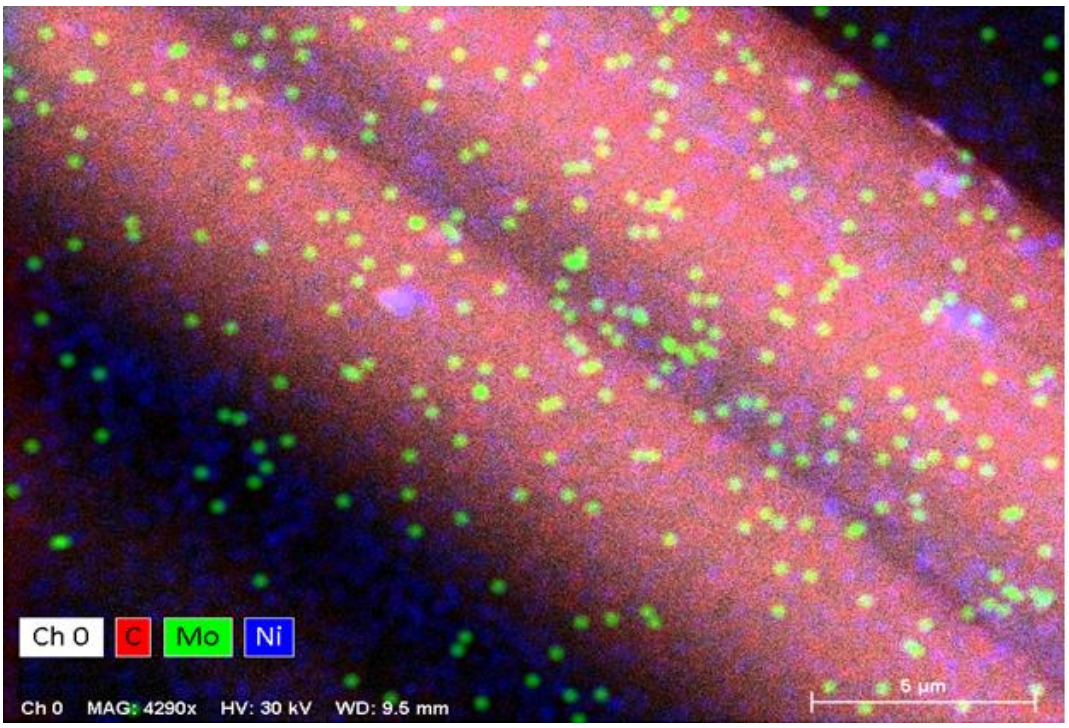

A

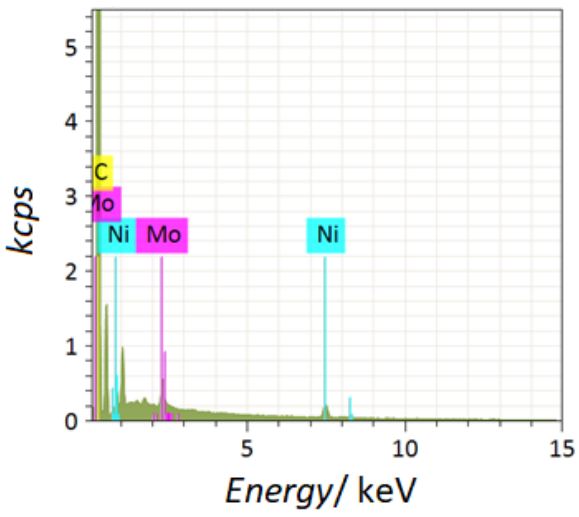

B

Figure 1. **a)** SEM micrograph picture with EDX mapping of MoNi/CF electrode, taken at 4,290× magnification, with an acceleration voltage of 30 kV; **b)** As above, but EDX spectrum.

Fig. 1a illustrates an arrangement of deposited MoNi alloy particles on the CF electrode, recorded at a magnification of 4,290×. Based on the micrograph picture, one can observe that the electrodeposition of MoNi alloy is quite homogeneous all over the CF electrode surface; however, the Mo deposit is concentrated in the form of chunks, while the Ni deposit is more uniformly distributed. Fig. 1b presents an EDX spectrum for the MoNi/CF surface, which allowed to calculate the average values of Mo and Ni content at 0.32 and 0.57 wt.%, correspondingly.

3.2. Oxygen evolution reaction on pure CF and oxidized MoNi/CF tow electrodes in 0.1 M NaOH solution

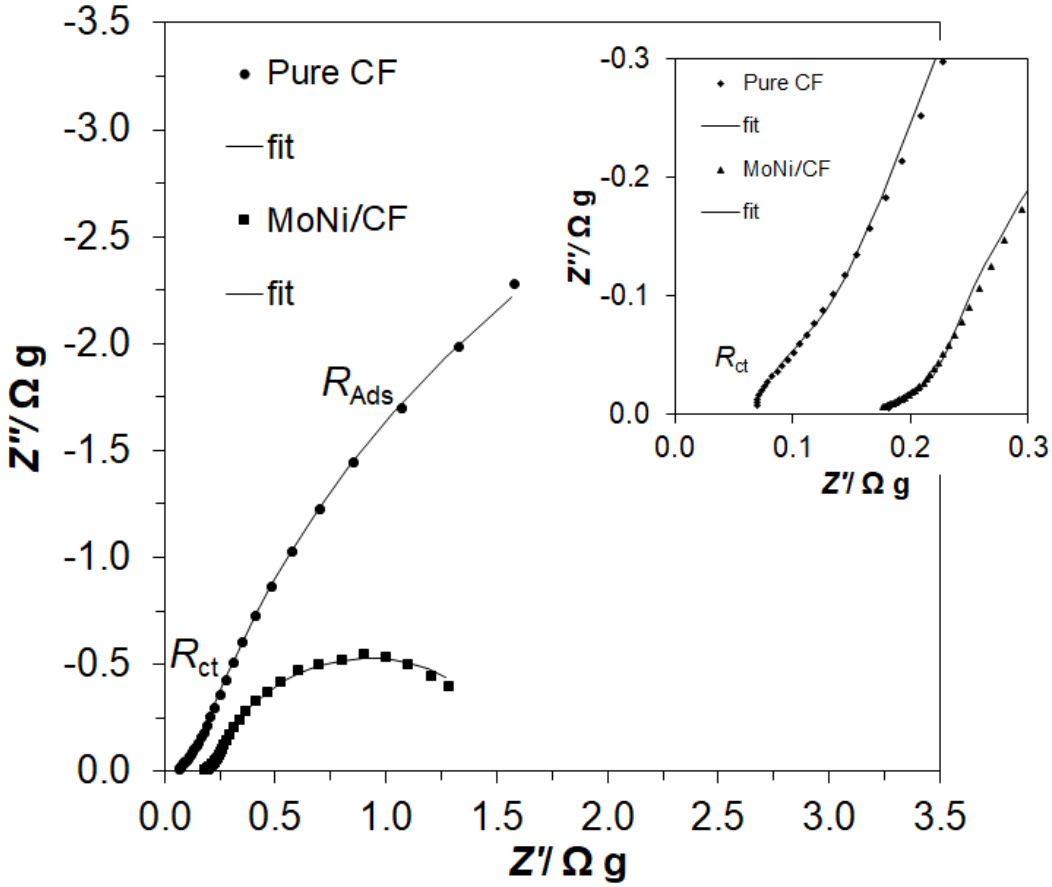

Figure 2. Complex-plane impedance plots for the OER on pure Hexcel 12K AS4C CF and MoNi/CF tow electrodes in contact with 0.1 M NaOH electrolyte, recorded at room temperature for the overpotential of 370 mV. The solid lines correspond to a representation of the data according to an equivalent circuit shown in Fig. 3.

The a.c. impedance behaviour of the OER recorded in 0.1 M NaOH for unmodified Hexcel 12K AS4C carbon fibre (pure CF) and MoNi/CF composite is presented in Fig. 2 and Table 1.

Table 1. Electrochemical parameters for the OER obtained at pure Hexcel 12K AS4C CF and MoNi/CF ox. tow electrodes in 0.1 M NaOH solution. The results were recorded by fitting the CPE-modified Randles equivalent circuit (Fig. 3) to the experimentally obtained impedance data (reproducibility usually below 10-15%, $\chi^2 = 2\times10^{-4}$ to 5×10^{-3}).

η/mV	R_{ct}/Ω g	C_{dl}/μF g^{-1} $s^{\varphi1-1}$	R_{ads}/Ω g	C_{ads}/μF g^{-1} $s^{\varphi2-1}$
Pure CF				
270	0.161 ± 0.006	186,883 ± 2,299	18.55 ± 2.17	355,513 ± 5,013
370	0.136 ± 0.004	137,692 ± 1,859	8.93 ± 0.40	354,100 ± 4,037
420	0.133 ± 0.005	133,588 ± 2,097	3.86 ± 0.09	346,150 ± 4,396
470	0.116 ± 0.004	99,854 ± 1,458	2.58 ± 0.05	344,154 ± 4,302
495	0.110 ± 0.003	93,475 ± 1,284	2.08 ± 0.03	347,413 ± 3,683
520	0.098 ± 0.003	82,571 ± 1,379	1.62 ± 0.02	353,533 ± 4,419
545	0.093 ± 0.002	75,663 ± 953	1.18 ± 0.01	365,758 ± 3,767
570	0.085 ± 0.002	66,346 ± 1,440	0.89 ± 0.01	374,504 ± 3,708
MoNi/CF				
270	0.080 ± 0.007	219,125 ± 7,998	10.62 ± 0.64	317,532 ± 10,320
370	0.058 ± 0.003	164,298 ± 5,000	1.41 ± 0.03	356,395 ± 9,765
420	0.053 ± 0.004	157,931 ± 7,549	0.66 ± 0.02	353,121 ± 9,005
445	0.050 ± 0.005	205,012 ± 11,003	0.50 ± 0.02	293,125 ± 7,651
470	0.049 ± 0.003	178,694 ± 5,215	0.41 ± 0.01	360,073 ± 8,570
495	0.049 ± 0.003	163,165 ± 8,501	0.40 ± 0.01	328,032 ± 10,923
520	0.048 ± 0.003	155,762 ± 7,399	0.38 ± 0.01	335,073 ± 16,854
570	0.046 ± 0.002	175,077 ± 8,334	0.37 ± 0.01	309,597 ± 11,981

At all examined potentials both electrodes exhibited two "depressed" partial semicircles over the high and low-frequency range (see examples of the recorded Nyquist impedance plots in Fig. 2). The electrochemical parameters for the OER were obtained by means of an equivalent circuit model (Fig. 3), which included two CPE-*R* elements. Thus, the high-frequency region corresponds to charge transfer resistance, R_{ct} and double-layer capacitance, C_{dl} for the OER, whereas the low-frequency region covers the adsorption of reaction intermediates on the electrode surface, R_{Ads} and pseudo-capacitance, C_{Ads} parameters [27].

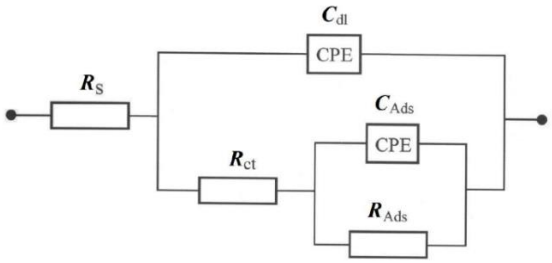

Figure 3. Equivalent circuit model used for fitting the impedance data for pure Hexcel 12K AS4C CF and MoNi/CF tow electrodes, obtained in 0.1 M NaOH solution. The circuit includes a constant phase element (CPE) for distributed capacitance; R_{ct} and C_{dl} elements correspond to the OER charge-transfer resistance and double-layer capacitance components; R_{Ads} and C_{Ads} parameters refer to the resistance imposed by the surface-adsorbed reaction intermediates and pseudocapacitance; R_{sol} is solution resistance.

Hence, it could be seen that the R_{ct} parameter value for pure CF sample decreased from 0.161 Ω g at the overpotential (η) of 270 mV to 0.085 Ω g at the overpotential of 570 mV. Moreover, the value of double-layer capacitance decreased from 186,883 μF g^{-1} $s^{\phi 1-1}$ to 66,346 μF g^{-1} $s^{\phi 1-1}$ for the same overpotential range. On the other hand, the MoNi/CF tow electrode presented *ca.* 2× smaller values of the R_{ct} parameter, which reached 0.080 Ω g and 0.046 Ω g at 270 mV, and 570 mV overpotential values, respectively. Although the C_{dl} value fluctuated throughout the examined overpotential range (see Table 1 for details), the overall trend was declining, reaching the highest value of 219,125 μF g^{-1} $s^{\phi 1-1}$ at η= 270 mV and the lowest of 155,762 μF g^{-1} $s^{\phi 1-1}$ at η= 520 mV. The above behaviour of the C_{dl} parameter, i.e. its reduction upon rising overpotential, could be explained by the partial blocking of the electrochemically active electrode surface by freshly-formed oxygen bubbles [11, 28].

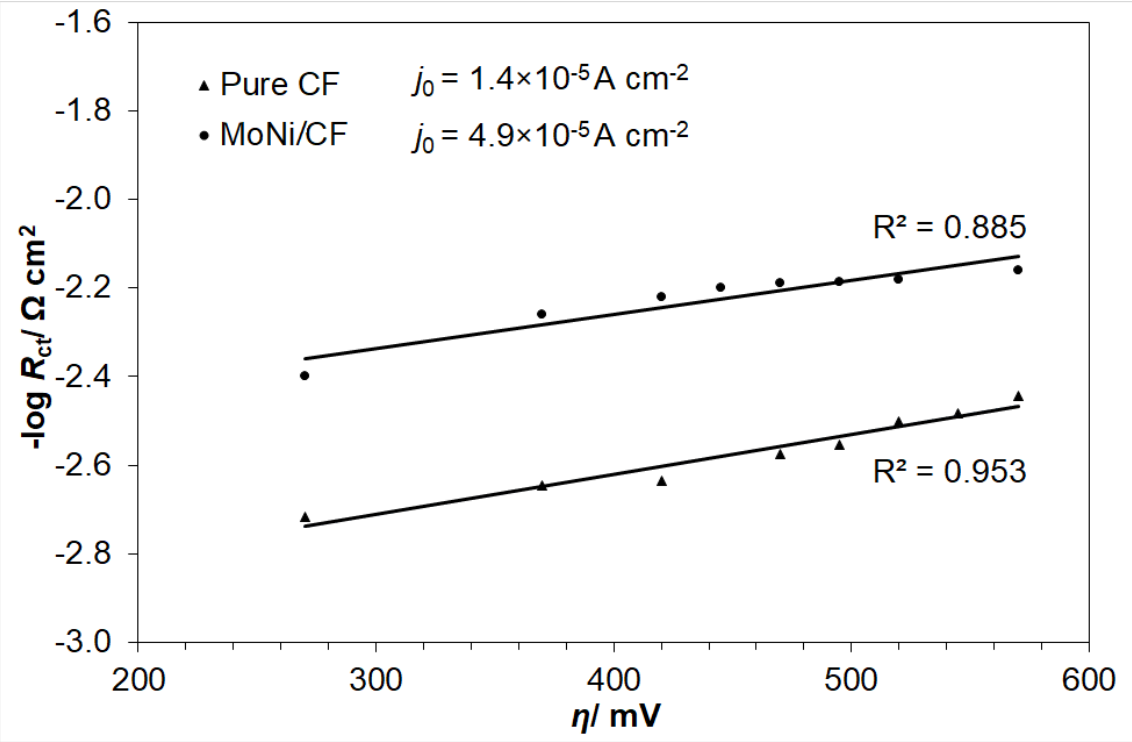

Figure 4. –log R_{ct} vs. overpotential relationship, obtained for the OER in 0.1 NaOH solution, for pure Hexcel 12K AS4C CF and MoNi/CF tow electrodes. Symbols represent experimental results and lines are data fits.

In addition, the linear relationship of –log R_{ct} vs. η (Fig. 4) refers to kinetically controlled process by the Volmer-Heyrovski route [29]. Based on this dependence and through utilization of the relation between the exchange current-density (j_0) and the R_{ct} parameter for overpotential approaching zero value [30,31], the values of j_0 were calculated for the examined electrodes by means of the Butler-Volmer equation. Hence, the obtained j_0 value for the studied overpotential range (η = 270-570 mV) came to 1.4×10^{-5} A cm^{-2} for pure CF tow material and 4.9×10^{-5} A cm^{-2} for the MoNi/CF electrode (3.5 times higher than that for the unmodified electrode). Furthermore, the potentiostatic Tafel polarization plots are presented in Fig. 5. Here, the corresponding Tafel-based values of the j_0 parameter for the OER came to 9.3×10^{-5} A cm^{-2} for pure CF sample and 6.7×10^{-4} A cm^{-2} for the MoNi/CF tow electrode, while the

recorded anodic Tafel slopes (b_a), approached 224 and 198 mV dec^{-1}, respectively. The significant difference between the Tafel-calculated and the impedance-derived values of the j_0 parameter for examined electrodes most likely results from lack of two typically well-defined linear regions of low and high overpotentials [28,32]. Moreover, with respect to the kinetic results discussed above, the Tafel-based data presented in this work should only be treated qualitatively.

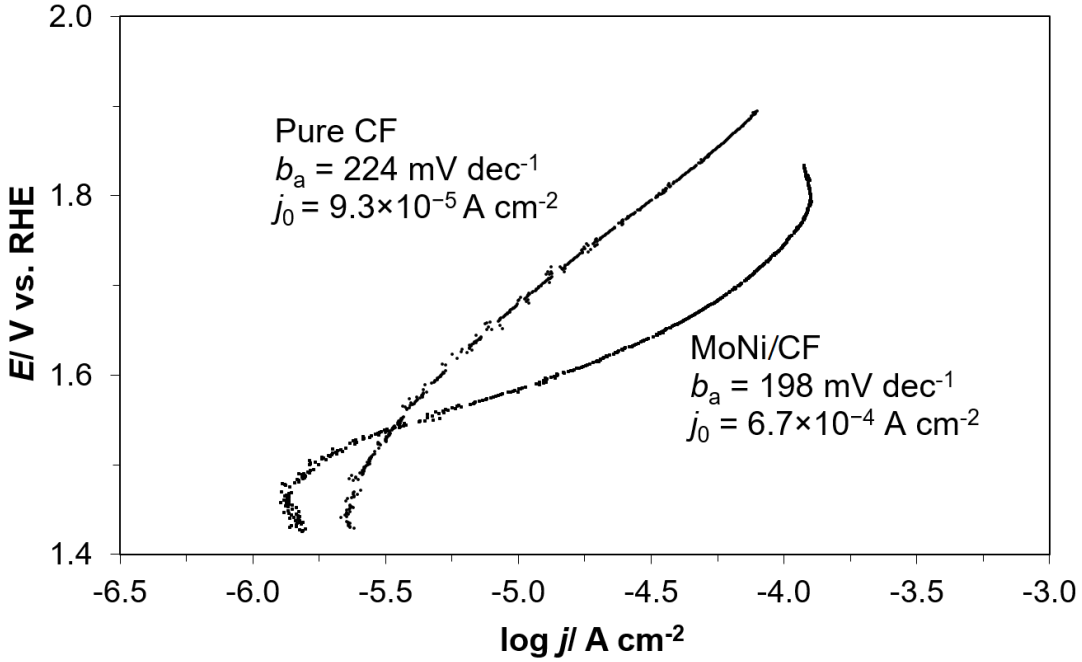

Figure 5. Quasi-potentiostatic anodic Tafel polarization curves (recorded at a scan-rate of 0.5 mV s^{-1}) for pure Hexcel 12K AS4C CF and MoNi/CF electrode surfaces, carried out in 0.1 M NaOH solution (appropriate *iR* correction was made based on the solution resistance derived from the impedance measurements); calculated Tafel slopes for pure CF and MoNi/CF materials came to b_a = 224 and 198 mV dec^{-1}, respectively.

The R_{ct}-derived exchange-current densities are somewhat lower compared to those of other OER works performed on MoNi alloys in alkaline solutions [28, 32]. Thus, the exchange current-density value recorded for Ni + Mo composite coating came to 9.7×10^{-5} A cm^{-2} in Ref. 28 and 5.2×10^{-5} A cm^{-2} in Ref. 32 for mechanically alloyed Ni and Mo powders on the electrode surface. However, taking into consideration that the NiMo alloy's loading did not exceed 2 wt.% of the electrode mass (compared to 99 wt. % for Refs. [28 and 32]) the electrode with a very small amount of NiMo alloy and slightly lower j_0 parameter value could be considered superior to those of bulk-type electrodes.

4. CONCLUSIONS

Low-level nickel and molybdenum deposits on the surface of carbon fibre material radically enhanced the catalytic activity of baseline material towards the anodic evolution of oxygen in an alkaline solution (especially observed over the kinetically-controlled overpotential range). The above is primarily

related to superior OER catalytic properties of MoNi alloy, in addition to the considerable modification of electrochemically-active surface for this catalyst material.

Finally, the results obtained in this work have shown that a small amount of MoNi alloy deposited on the materials with large electrochemically active surface area, such as carbon fibre, not only could significantly facilitate of the OER performance, but also replace expensive materials by a cheaper analogue for the mass production in commercial alkaline water electrolysers.

ACKNOWLEDGEMENTS
The authors would like to thank the Team of Erasmus+ Water Project No. 561755-EPP-1-2015-1-NOEPPKA2-BHE-JP for supporting our research and cooperation in the frame of our Erasmus+ Student Mobility Program.

FUNDING
This work was financed by the internal research grant of The University of Warmia and Mazury in Olsztyn, project no. 20.610.001-300.

References

1. F. Sorgulu and I. Dincer, *Int. J. Hydrogen Energy*, 43 (2018) 5842–5851.
2. M.E. Demir and I. Dincer, *Int. J. Hydrogen Energy*, 47 (2017) 30044–30056.
3. M. Carmo, D.L. Fritz , J. Mergel and D. Stolten, *Int. J. Hydrogen Energy*, 38 (2013) 4901–4934.
4. O. Schmidt, A. Gambhir, I. Staffell, A. Hawkes, J. Nelson and S. Few, *Int. J. Hydrogen Energy*, 42 (2017) 30470–30492.
5. A. Gomez Vidales, K. Choi and S. Omanovic, *Int. J. Hydrogen Energy*, 43 (2018) 12917–12928.
6. J. Jiang, A. Zhang, L. Li and L. Ai, *J. Power Sources*, 278 (2015) 445–451.
7. Y. Zhang, Q. Shao, S. Long and X. Huang, *Nano Energy*, 45 (2018) 448–455.
8. M. Tahira, L. Pana, F. Idreesd, X. Zhanga, L. Wanga, J.-J. Zoua and Z. L. Wang, *Nano Energy*, 37 (2017) 136–157.
9. M. Gong and H. Dai, *Nano Research*, 8 (2015) 23–39.
10. Y. Guo, D. Guo, F. Ye, K. Wang and Z. Shi, *Int. J. Hydrogen Energy*, 42 (2017) 17038–17048.
11. B.M. Jović, U.Č. Lačnjevac, V.D. Jović, Lj. Gajić-Krstajić, J. Kovač, D. Poleti and N.V. Krstajić, *Int. J. Hydrogen Energy*, 41 (2016) 20502–20514.
12. A. Eftekhari, *Materials Today Energy*, 5 (2017) 37–57.
13. J.-M. Hu, J.-Q. Zhang, C.-N. Cao, *Int. J. Hydrogen Energy*, 29 (2004) 791–797.
14. I.A. Lervik, M. Tsypkin, L.-E. Owe and S. Sunde, *J. Electroanal. Chem*., 645 (2010) 135–142.
15. L.-E. Owe, M. Tsypkin, K.S. Wallwork, R.G. Haverkamp and S. Sunde, *Electrochim. Acta*, 70 (2012) 158–164.
16. E. Tsuji, A. Imanishia, K. Fukuia and Y. Nakato, *Electrochim. Acta*, 56 (2011) 2009–2016.
17. Z. Lu, H. Wang, D. Kong, K. Yan, P.-C. Hsu, G. Zheng, H. Yao, Z. Liang, X. Sun and Y. Cui, *Nature Communications*, 5 (2014) 4345.
18. M.E.G. Lyons and M.P. Brandon, *J. Electroanal. Chem*., 631 (2009) 62–70.
19. T. Wang, W. Xu and H. Wang, *Electrochim. Acta*, 257 (2017) 118–127.
20. F.J. García-Mateos, T. Cordero-Lanzac, R. Berenguer, E. Morallón, D. Cazorla-Amorós, J. Rodríguez-Mirasol and T. Cordero, *Appl. Catal., B*, 211 (2017) 18–30.

21. J.-Q. Chi, K.-L. Yan, Z. Xiao, B. Dong, X. Shang, W.-K. Gao, X. Li, Y.-M. Chai and C.-G. Liu, *Int. J. Hydrogen Energy*, 42 (2017) 20599–20607.
22. H.J. Seim and M.L. Holt, *J. Electrochem. Soc*., 96 (1949) 205.
23. J.R. Macdonald, Impedance Spectroscopy, Emphasizing Solid Materials and Systems, John Wiley & Sons, Inc., New York (1987).
24. B. Pierozynski, T. Mikolajczyk and I.M. Kowalski, *J. Power Sources*, 271 (2014) 231–238.
25. B. Pierozynski and T. Mikolajczyk, *Electrocatalysis*, 6 (2015) 51–59.
26. T. Mikolajczyk and B. Pierozynski, *Int. J. Electrochem. Sci.*, 13 (2018) 621–630.
27. F.R. Costa, D.V. Franco and L.M. Da Silva, *Electrochim. Acta*, 90 (2013) 332–343.
28. J. Kubisztal and A. Budniok, *Int. J. Hydrogen Energy*, 33 (2008) 4488–4494.
29. B.E. Conway and B.V. Tilak, *Adv. Catal.*, 38 (1992) 1.
30. J.G. Highfield, E. Claude and K. Oguro, *Electrochim. Acta*, 44 (1999) 2805.
31. R.K. Shervedani and A.R. Madram, *Electrochim. Acta*, 53 (2007) 426.
32. M. Plata-Torres, A.M. Torres-Huerta, M.A. Domínguez-Crespo, E.M. Arce-Estrada and C. Ramírez-Rodríguez, *Int. J. Hydrogen Energy*, 32 (2007) 4142–4152.